Binaural simulation of concert halls: A new approach for the binaural reverberation process

J. Martin, D. Van Maercke, and J-P. Vian
Centre Scientifique et technique du batiment (C.S.T.B.), 24, rue Joseph Fourier, 38400 Saint Martin D'heres, France

(Received 24 June 1992; revised 6 July 1993; accepted 16 July 1993)

A geometrical cone-tracing method associated with the signal processing technique is used to calculate the binaural impulse response of a concert hall. Some inaccuracy and the computation time of the geometrical algorithm tend to limit the method for the high-reflection orders which are necessary to provide a good listening effect. In order to extend the response, a new approach is presented based on different statistical processes that depend on both the acoustical and geometrical characteristics of the hall. After a theoretical presentation (new statistical results are proposed to describe the sound field behavior in a concert hall), some simulations are given in order to illustrate the different statistical processes. This simulation technique seems to be a very convenient tool both for the design of a new concert hall and for the study of the important parameters in auditory spaciousness.

PACS numbers: 43.55.Fw, 43.55.Hy, 43.55.Lb

INTRODUCTION

Simulation of listening impressions has become more and more important for the acoustical planning of a new concert hall prior to building. Over the last few years, monophonic predictions have already been performed,[1] but fully realistic simulations can only be obtained if the auditory spaciousness is reproduced correctly. All of this leads to the prediction of concert hall binaural impulse response (including head directivity) on which this paper is focused. When the binaural response is known, convolution with anechoic recordings provides the listening tests.

The proposed algorithm uses a geometrical approach associated with a new statistical method which provides two artificial reverberation processes (left and right ears) in order to extend the binaural response. The mixing of geometrical and statistical procedures has been involved because of the shortcomings introduced by a purely geometrical method when predicting the late response.

The problem of artificial reverberation has been studied for a long time[2–4] and several forms of recirculating delay reverberators have been proposed. They can be constructed as electronic units. Meanwhile, it has been shown that such systems produce some "anonymous" reverberation, which is far from the response of the actual room under analysis. (These electronic reverberators do not take into account the geometrical characteristics and the exact coloration due to the material used.) In Ref. 5, it was proposed that we use the image source method to estimate the early reflections with recirculating delays for the late response. This does not solve the problem of giving the exact coloration of the room to the reverberation process. This is the first point tackled herein.

The second point concerns the generation of binaural signals. Many recent works have been carried out on this subject.[6–8] The subjective preference of concert hall versus auditory spaciousness has also induced many studies,[9,10] and the design policy of recent concert halls seems to follow these results. It is assumed that auditory spaciousness is strongly related to early lateral reflections[11] and reverberation.[10] Thus an efficient prediction method must take into account both the exact early lateral reflections and the exact reverberation.

I. DESCRIPTION OF THE METHOD

A room impulse response can be regarded as being composed of three parts, depending on the number of acoustical events that occur and can be separated according to the reflection order considered. The first part corresponds to the direct sound and the early reflections (low-reflection orders) where the event's behavior is purely deterministic. In contrast, the third part corresponds to reverberation (high-reflection orders) where the events are randomly distributed. Between these two parts, the phenomena behave as a mixture of both deterministic and random processes. Following this physical scheme, the computation of the impulse response is performed in three parts.

Part 1: Calculation of the direct sound and the early reflections according to a geometrical approach (order 0 to $n_{geo}=4$ or 6): The different acoustical paths between the source and the listener's head position are determined by a geometrical cone method.[12] Then, the physical elements such as the directivity of the sources, the outer ear transfer functions, the absorption at the boundaries, and the air absorption are taken into account as individual linear filters.

Part 2: Calculation of the beginning of the reverberation process according to a "pseudo-statistical" approach (order 4 or 6 to $n_{ps}=10$ or 15): The calculation is done in the same way as for the first part except that the following parameters (which are used in the geometrical approach) are set up by random trial or linear prediction: (1) the

 0001-4966/93/94(6)/3255/10/$6.00

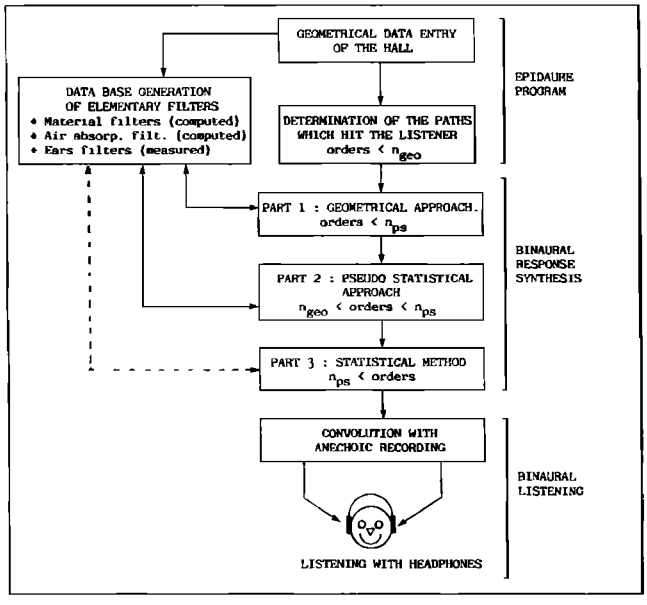

FIG. 1. General block diagram of the algorithm.

number of possible paths between the source and the auditor for a given reflection order n, (2) the lengths of these paths, (3) the set of collision surfaces for each path (the surfaces that are concerned with each path), (4) the azimuth and elevation of the directions of the cones starting from the source, and (5) the azimuth and elevation of the directions of the cones arriving at the listener's head.

Part 3: Calculation of the last part of the response according to a purely statistical approach (order > 10 to 15).

For these high-reflection orders it is considered that the number of paths is large enough that the density of reflection can be substituted for each ear by time variant filtered white noise.

The time variant filter characteristics and the cross correlation coefficient of the two noises are deduced from parts 1 and 2 of the impulse responses in such a way that they depend on the hall geometry and materials. Figure 1 gives the general block diagram of the proposed algorithm.

II. CALCULATION OF THE FIRST PART OF THE BINAURAL IMPULSE RESPONSE: THE GEOMETRICAL APPROACH

This approach is divided into three parts.[12] First of all, the acoustical paths that reach the listener are determined. Then, the linear filters corresponding to the physical elements mentioned above are calculated and stored in a database. Finally, the impulse response of each path is synthesized and added to provide the binaural response.

A. Determination of the paths between the source and the listener

This work is entirely done by the EPIDAURE program developed by the Centre Scientifique et Technique du Bâtiment (C.S.T.B.) in recent years. This program is organized as a tool box with many applications beginning by the entry of geometrical data set describing the room and the different acoustical parameters (relative humidity, temperature, acoustical characteristics of the surfaces, source, and listener locations, etc.). Then, the cone-tracing algorithm produces the different paths between the sources and the listeners with their history: starting and arrival angles, arrival times, collision surfaces. Each path first found by the program is checked by retropropagation of a ray from the listener to the source. Thus no wrong path can occur. The method presents some limitations which justify the use of statistical methods. We shall discuss this problem more precisely later.

B. Database generation of elementary filters

As previously stated, the intervening acoustical modifications during the propagation of each cone are transformed into realizable linear filters. The first step consists of interpolating the modulus transfer function of the material reflection coefficients and the modulus transfer function values of the source directivities (spline cube interpolation on the modulus), which are generally known in octave bands. Although frequently used, this method that gets the value of the filter transfer function modulus over all frequencies is not strictly correct. That is, the resulting absorption coefficients, derived from the filters, differ from the original ones. The reason is that the original absorption coefficient represents a mean value over a certain frequency band and not at a single frequency, as it is assumed in the interpolation method (the source directivities are described by octave bands in two perpendicular planes; a spatial interpolation provides 3-D directivities).

The modulus of the air absorption transfer function is directly computed according to Ref. 13. Let $|h(f)|$ denote the interpolated values over all frequencies of the modulus. Here, $|h(f)|$ is a real function without any phase component. This corresponds in the time domain to a filter which is both nonreal and noncausal. Thus a function $h(f)$ must be derived with the same spectral characteristics but with a real and causal impulse response. In other words, a phase component $\phi(f)$ must be determined to fulfill this objective. Then, the final filter transfer function is

$$h(f)=|h(f)|e^{j\Phi(f)}. \tag{1}$$

In this sense, $h(f)$ is defined as the transfer function of a minimum phase filter which guarantees the causality constraint.[14] The logarithmic formula of the Bayard–Bode relations provides the phase component,

$$\Phi(f)=\mathrm{HT}[\log|h(f)|], \tag{2}$$

where HT[ ] denotes the Hilbert transform and $\mathrm{Sgn}(t)$ is the sign pseudofunction. Then, $h(f)$ is easily deduced from Eq. (1). The negative frequency values are computed by Hermitian symmetry:

$$h(-f)=h^*(f), \tag{3}$$

which fulfills the real constraint (h^* denotes the complexe conjugate of h).

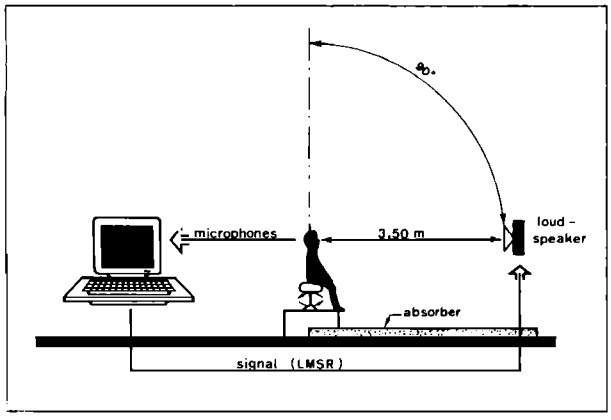

(a)

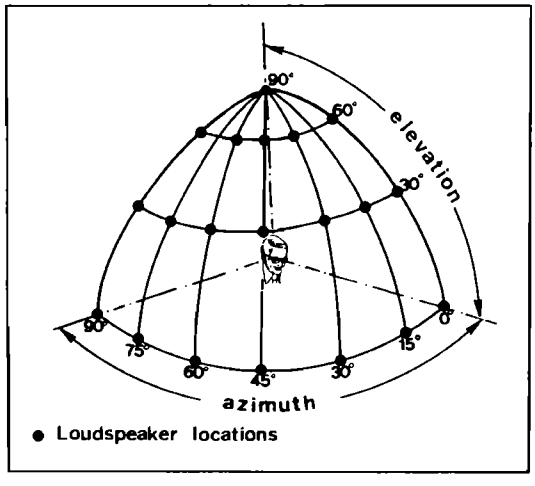

(b)

FIG. 2. (a) The head related transfer functions (HRTF) measurement system. (b) Successive locations of the loudspeaker on a quarter of a hemisphere. The whole hemisphere has been explored.

The database will be complete if it contains some kind of filter that represents the head directivity. For this, head related transfer functions (HRTF) have been measured first by time delay spectrometry, and more recently by a cross-correlation method using linear maximal shift register sequences and time windowing. Both of the methods run on a personal computer.[15,16] Figure 2(a) shows the measuring system. The receiver is composed of two electret microphone capsules located at the ear canal entrances. The measurement arrangement makes the use of a 20-ms free-field time window possible, which ensures a 50-Hz frequency resolution. (As the quality of the absorber becomes bad at low frequencies, the ground reflection response can damage the desired direct response. In such a case, the samples corresponding to the ground reflection response are set to zero. Then, using an autoregressive extrapolation method,[17] the corresponding time interval is rebuilt according to the time and frequency characteristics of the direct path response.) Some improvements have been introduced compared to the experiment described in Ref. 13. The sample frequency is 40 kHz with 1024 temporal samples (20 kHz before), and 61 angles of incidence have been measured [cf. Fig. 2(b)]. As the auditor generally looks at the source, the chosen HRTF of the lower hemisphere is identical to those measured with 0° in elevation but with a 6-dB attenuation from $-15°$ to $-90°$ in elevation.

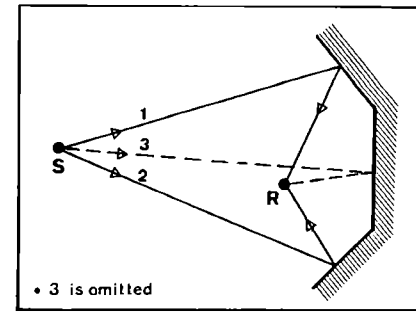

FIG. 3. Example of a missed path.

C. Synthesis of the first part of the response: Geometrical synthesis

The geometrical part of the binaural impulse response is calculated according to the following sequence.

(1) For each path i with associated delay τ_i, compute the transfer function of source directivity using the starting angles of the rays, select the correct right and left ear transfer functions corresponding to the arriving angles, compute the product of the successive transfer functions (source) $\times$(reflection on the surfaces)$\times$(air absorption)$\times$(left ear; right ear), and compute the inverse Fourier transform to obtain the two impulse responses of path i: $R_i(t)$, $L_i(t)$.

(2) Sum up all path impulse responses with the correct associated delays: $R(t)=\Sigma_i R_i(t-\tau_i)$ (right ear) and $L(t)=\Sigma L_i(t-\tau_i)$ (left ear).

D. Limitations of the geometrical approach

The first kind of limitation lies in the inaccuracy of the method due to the spatial sampling. In order to be propagated, the cones are assimilated to their symmetry axes. The spacing between two axes increases with the distance from the source so that some paths can be missed when a surface is small enough to be situated between two consecutive axes. This is shown in Fig. 3. Thus the higher the order of the geometrical reflection, the shorter the angle between two axes must be. Consequently, the number of cones increases and so does the computation time (as the length of a path tends to increase with the reflection order, this problem becomes crucial for high values of n). The second kind of limitation arises from the fact that the computation time increases with the 3th power of the order of reflection. Practically, the above-mentioned problems tend to limit the geometrical approach to orders lower than four or six. Of course it is not sufficient to provide a realistic listening impression. Thus a statistical method has been introduced to extend the impulse response.

III. CALCULATION OF THE SECOND PART OF THE BINAURAL IMPULSE RESPONSE: THE PSEUDOSTATISTICAL APPROACH

The basic principle of the geometrical approach is used except that the acoustical characteristics of the paths are determined according to some appropriate random process.

A. Determination of the relevant statistical parameters

For a given order n, the following parameters have to be predicted: (1) the number of image sources of order n, (2) the length of each of the paths between the image sources and the listener, (3) the n successive intervening surfaces on which the image sources are supposed to be taken, and (4) the starting and arriving angles of the paths.

IV. ESTIMATION OF THE NUMBER OF IMAGE SOURCES

Let $f(n)$ be the number of image sources for the order n since the geometrical approach has run up to the order n_{geo}, then the values of $f(k)$, $k=0,\ldots,n_{\text{geo}}$, are used to predict $f(k)$ for $k>n_{\text{geo}}$.

The following assumption has to be made for $f(n)$:

$$\lim_{n\to+\infty}\frac{f(n)}{n^2}=A, \tag{4}$$

where A takes a finite value. This expresses the energy stabilization in a perfectly reverberant room, where the energy coming from each image source is proportional to $1/d^2$, hence $1/n^2$.

Many extrapolation techniques have been empically tested. The best fit found (accuracy and robustness) has been obtained with the assumption of parity for $f(n)$ and $f(0)=2$ [for a parallelepipedal room the exact solution is $f(n)=4n^2+2$ $n\geqslant 1$] (Ref. 18). Then the extrapolated solution form is

$$f(n)=an^2+2, \tag{5}$$

and a is determined by using a least-mean squares method on $f(n)$, $n\leqslant n_{\text{geo}}$. This seems to be the most robust method against fluctuations in $f(n)$.

V. ESTIMATION OF THE LENGTH OF AN nth-ORDER PATH BETWEEN AN IMAGE SOURCE AND THE LISTENER

The $f(n)$ values of the nth-order paths distance are obtained by random trials according to a probability density function for n. Let $P_n(r)$ be the distribution function of the length r for an nth-order path which reaches the listener. It can be shown (see Appendix A) that $P_n(r)$ can be expressed in the following terms:

$$P_n(r)=\frac{r^2}{\sqrt{2\pi n\sigma_{\bar{l}}^2(n\sigma_{\bar{l}}^2+n^2\bar{l}^2)}}\exp\left(-\frac{1}{2}\frac{(r-n\bar{l})^2}{n\sigma_{\bar{l}}^2}\right). \tag{6}$$

The mean-free path $\bar{l}$ and the variance $\sigma_{\bar{l}}^2$ can be estimated from the lengths r_i of the paths between the image sources and the listener obtained in the geometrical approach (for the highest order n_{geo}):

$$\bar{l}=\frac{1}{n_{\text{geo}}}=\frac{\sum_{i=1}^{f(n_{\text{geo}})}(1/r_i^2)r_i}{\sum_{i=1}^{f(n_{\text{geo}})}(1/r_i^2)}, \tag{7}$$

$$\sigma_{\bar{l}}^2=\frac{R^2-(n_{\text{geo}}\bar{l})^2}{n_{\text{geo}}}, \tag{8}$$

with

$$R^2=\frac{\sum_{i=1}^{f(n_{\text{geo}})}(1/r_i^2)r_i^2}{\sum_{i=1}^{f(n_{\text{geo}})}(1/r_i^2)}.$$

Since the estimation is calculated on the restricted class of the paths which reach the listener and not over all of them, the weighting term $1/r_i^2$ is necessary (the $1/r_i^2$ weighting is not necessary when the estimation of $\bar{l}$ and $\sigma_{\bar{l}}^2$ is made over all the paths starting from the source). This also supposes that the n_{geo}-order path length is composed of n_{geo} independent elementary path lengths.

Now, some empirical contributions to the statistical parameters used in Eq. (8) must be considered. Let $\overline{ln}$ be the mean cumulative length of an nth-order path, and σ_{ln}^2 be the corresponding cumulative variance.

In the analytical development carried out in Appendix A, the results presented in Ref. 19 are used. Here, $\overline{ln}$ and σ_n^2 are expressed in the following way:

$$\begin{aligned}\overline{ln}&=n\bar{l},\\ \sigma_{\overline{ln}}^2&=n\sigma_{\bar{l}}^2.\end{aligned} \tag{9}$$

Some modifications must be introduced according to the results of a statistical study summarized herein.

Figure 4(a) and (b) shows, respectively, $\bar{l}_n$ vs n and $20\log(\sigma_{\overline{ln}})$ vs n in the room presented in Fig. 4(c). These results have been obtained using the geometrical cone algorithm with a high resolution (1 deg between each cone axis).

It can be seen [Fig. 4(a)] that $\bar{l}_n$ is a linear function versus n but with a nonzero ordinate at the origin and not simply $n\bar{l}$. The origin ordinate and the slope must be estimated by a geometrical approach.

In a similar way, the logarithm of $\sigma_{\overline{ln}}$ presents the same kind of variation as $\bar{l}_n$ vs n [Fig. 4(b)]. This means that the cumulative variance can be described by the following expression:

$$\sigma_{\overline{ln}}^2=n^{\alpha}\sigma_{\bar{l}}^2, \tag{10}$$

where α must be estimated in the geometrical approach, and we have found that α always lies between 1 and 2.

Many tests have been performed on others rooms: they confirm these results. So the law finally chosen is

$$P_n(r)=\frac{r^2}{\sqrt{2\pi\sigma_{\overline{ln}}(\sigma_{\overline{ln}}^2+\bar{l}_n^2)}}\exp\left(-\frac{1}{2}\frac{(r-\overline{ln})^2}{\sigma_{\overline{ln}}^2}\right),$$

$$\sigma_{\overline{ln}}^2=n^{\alpha}\sigma_{\bar{l}}^2,\quad \alpha\in[1,2]. \tag{11}$$

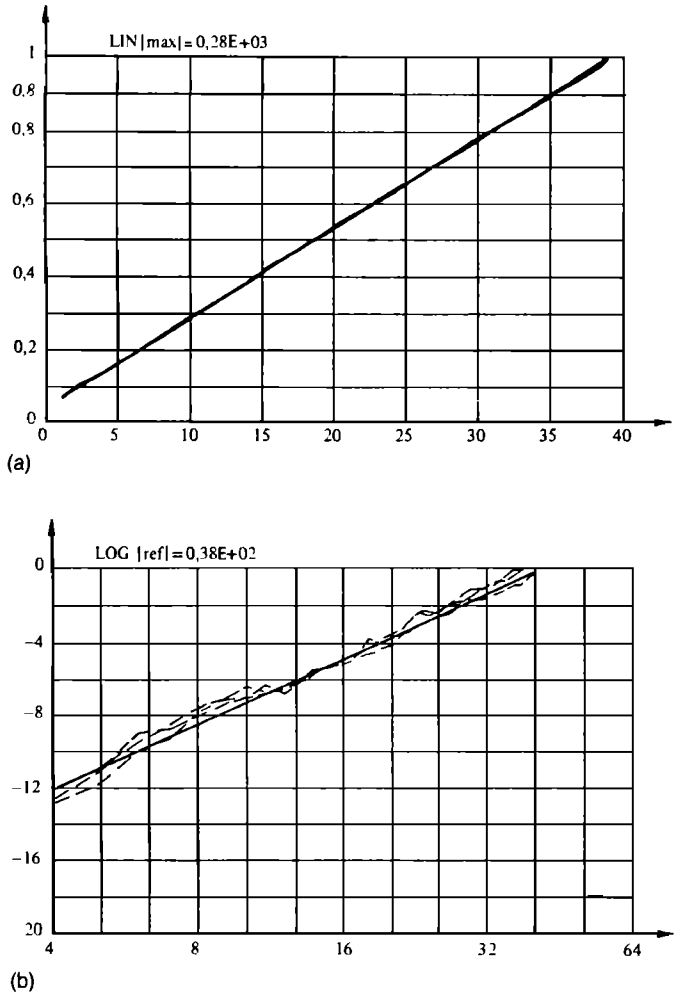

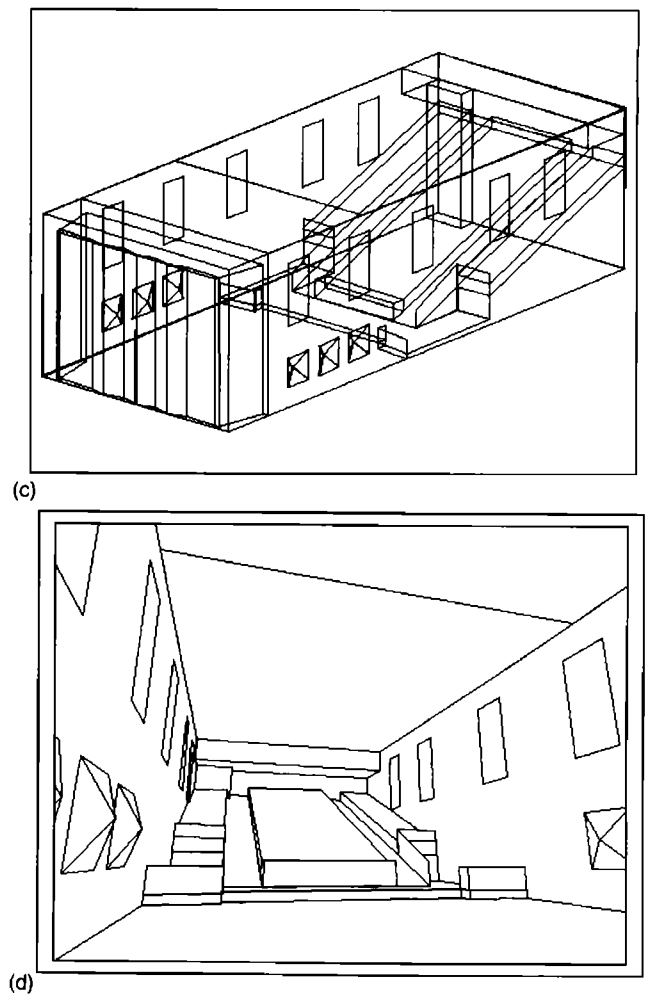

FIG. 4. (a) Mean cumulative length of an nth-order path versus n. (b) 20 log (mean cumulative variance) versus n. (c) General arrangement of the hall (Olivier Messiaen Hall in Grenoble). (d) Inside view of the hall (Olivier Messiaen Hall in Grenoble).

VI. DETERMINATION OF THE n SUCCESSIVE INTERVENING SURFACES FOR AN nth-ORDER PATH

The n successive intervening surfaces corresponding to a given path are randomly determined according to the collision probabilities on the surfaces. These probabilities are estimated during the geometrical approach. The collision frequency f_{S_i} of a surface s_i is computed as follows:

$$f_{S_i} = n_{S_i} \Big/ \sum_{i=1}^{S_{\max}} n_{S_i}, \tag{12}$$

where n_{S_i} represents the number of collisions on the surface S_i for all the reflection orders $[1,.,n_{\text{geo}}]$ and $S_{\max}$ is the number of surfaces.

As $\Sigma_{i=1}^{S_{\max}} f_{S_i} = 1$, and f_{S_i} is independent of the chosen value for n_{geo}, the collision probabilities are taken to be equal to the collision frequencies. It has been shown[20] that the collision probability of a surface is simply the area of surface divided by the sum of all areas. This is well verified in a diffuse sound field. In the program presented here, it is easier to determine the collision probabilities by a statistical determination as it is necessary to propagate the cones. This avoids the computation of all the surface areas of the room and is more accurate for nondiffuse fields.

VII. ESTIMATION OF THE STARTING/ARRIVING ANGLES OF THE PATHS

For each path, the set of intervening surfaces is randomly selected according to the previously determined collision properties. The starting direction of the path (azimuth and elevation) is taken as the direction of the line which links the source and the center of gravity of the first surface of the set. In the same way, the arriving direction is taken as the direction of the line running from the center of gravity of the last surface randomly selected to the listener.

A. Pseudostatistical synthesis

The algorithm is very similar to the one used in the geometrical approach. It can be summarized as follows: For $n > n_{\text{geo}}$, compute the number of paths $f(n)$ according to Eq. (5); compute $f(n)$ random trials according to Eq. (11) in order to find the lengths of the $f(n)$ paths, compute $f(n)$ random trials according to Eq. (12) in order to find the $f(n)$ sets of n collision surfaces, for each set of surfaces, compute the arriving/starting angles, and connect to the geometrical synthesis algorithm using the previous predicted parameters.

This method permits avoidance of the geometrical approach and its associated accuracy limitation, and reduces

the time computation of the determination of the paths. However, the overall computation time of the last step of the algorithm still increases with the order of reflection in a similar way as for the geometrical approach (the running mode is always "path by path"). Practically, it is used for reflection orders up to 10 or 15 which has been proved during listening tests not to be enough to produce really natural sound. As the sound field becomes more and more diffused versus the order of reflection, a purely statistical method can be used to predict the tail of the response.

VIII. PREDICTION OF THE TAIL OF THE RESPONSE : THE STATISTICAL APPROACH

For high orders of reflection, it can be considered that the density of contributions reaching the listener is so large that it can be modeled by some time-frequency windowed Gaussian white noise. (The required values for the reflection density lie within the range of 250 to 2800 s^{-1}.) It is no longer necessary to look to the determination of the collision surfaces set or the starting/arriving angles as far as the time-frequency characteristics of the noise are related to the hall characteristics.

Two different white noises must be used, one for the left ear and the other for the right ear. Now, we discuss the following points: how to choose the time window, how to choose the frequency window, and how to generate the two white noises such that the interaural cross correlation is adjusted to the right value.

A. Frequency windowing

Kuttruff has shown[19] that in a space composed only of two surfaces $S1$ and $S2$, the expectation value of the sound particle energy after N collisions can be written as

$$\langle E_N \rangle = E_0(1-\bar{\alpha})^N, \tag{13}$$

where $\bar{\alpha}$ represents the mean absorption coefficient of $S1$ and $S2$. By using the multinomial law, this result can be easily extended to a room including $S_{\max}$ surfaces. So we can define a mean reflection filter of the room at the order n, $r_n(f)$ such that

$$|r_{n(f)}|^2 = [1-\bar{\alpha}(f)]^n,$$

with

$$\bar{\alpha}(f) = \sum_{i=1}^{S_{\max}} f_{S_i} \alpha_{S_i}(f). \tag{14}$$

Here, f_{S_i} is given by Eq. (11) and f denotes the frequency [it can be noted that by using the fact that the collision frequency is proportional to the area of the surface in a diffuse sound field, Eq. (14) turns out to be Sabine's formula for the average absorption coefficient].

Two other frequency windows are used. The first one includes the mean air absorption effect. For nth-order path contribution, we use the air absorption filter calculated for a mean propagation distance equal to l_n. The second one includes the effect of a mean ear filter over the ear filters selected in the previous approaches. Note that in the algorithm the frequency windowing is applied before the time windowing.

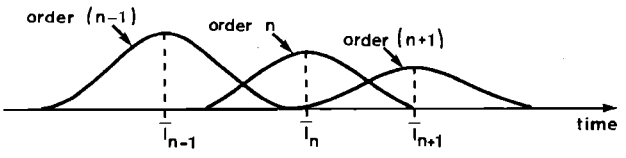

FIG. 5. Evolution of the time windows $H_n(t)$ versus the reflection order n.

B. Time windowing

Let $B(t)$ be a Gaussian white noise and $H_n(t)$ be the time window. If $K_n(t)$ denotes the instantaneous mean power of the nth-order paths which reach the listener at time t,

$$\sigma^2_{\mathrm{BH}}(t) = K_n(t),$$

where $\sigma^2_{\mathrm{BH}}(t)$ equals the variance of the H-windowed white noise and $K_n(t)$ is proportional to $P_n(t) \cdot E_{\mathrm{ray}}(t)$ where $P_n(t)$ is the nth-order ray collision probability on the listener and $E_{\mathrm{ray}}(t)$ is the mean energy of a ray at time t. Here, $P_n(t)$ has been computed and is given by Eq. (11). As is well known, in a reverberant room,

$$E_{\mathrm{ray}}(t) = k/t^2 \quad \text{(geometrical divergence of a ray)}.$$

By combining these results, $K_n(t)$ can be written as

$$K_n(t) = k' \exp\left(-\frac{1}{2} \frac{(ct-\bar{l}_n)^2}{n\sigma^2_{\bar{l}}} \right) \tag{15}$$

and $H(t)$ is easily deduced from (15) [$H(t)$ must be in terms of pressure],

$$H_n(t) = k_0 \left[\exp\left(-\frac{1}{2} \frac{(ct-\bar{l}_n)^2}{n\sigma^2_{\bar{l}}} \right) \right]^{1/2}. \tag{16}$$

Figure 5 illustrates the time windowing operation versus the successive reflection.

C. Interaural cross correlation (IACC)

Much work has been reported on the interaural cross correlation.[21,22] The two signals received by the right and the left ears are neither uncorrelated nor proportional. The value of the IACC must be respected in order to restore the true spatial impression. Let $B_R(t)$ and $B_L(t)$ be, respectively, the two white noises used for the right and left ears. It has been empirically established that the value of IACC computed from the impulse responses remains constant versus the order n if $n > 6$ or 7. (This does not remain true in the early part of the impulse response, when $n < 6$.) Thus the IACC is first estimated over the simulated response computed in the pseudo-statistical method; then the $B_R(t)$ and $B_L(t)$ are correlated according to this estimated value as follows.

Let $B_1(t)$ and $B_2(t)$ be two independent white noises:

$$B_R(t) = \cos\theta\, B_1(t) + \sin\theta\, B_2(t),$$

$$B_L(t) = \sin\theta\, B_1(t) + \cos\theta\, B_2(t), \qquad (17)$$

$$\theta = \tfrac{1}{2}\arcsin\ (\mathrm{IACC}).$$

The last problem is to calculate the coefficient k_0 in Eq. (16) in order to adjust the amplitude of the pseudostatistical process to the statistical process. This is done by calculating the energies of the right and left responses $(E_R n_{ps}, E_L n_{ps})$ on the last order (n_{ps}) of the pseudostatistical process. Then, K_0 is determined according to $E_R n_{ps}$ and $E_L n_{ps}$ taking into account the the mean absorption filter and the air absorption filter corresponding to the difference $n - n_{ps}$. These operations are detailed in Appendix B.

D. Statistical synthesis

The algorithm can be summarized by the following sequence.

(1) For $n_i > n_{ps}$, generate two independent Gaussian white noises $B_1(t)$, $B_2(t)$—add up the contributions of the order n_i; and compute $B_R(t)$ and $B_L(t)$ according to the IACC estimated on the pseudostatistical method.

(2) For each order n_i, compute the frequency windowing of the B_R and B_L according to Eq. (14), compute the time windowing of B_R and B_L according to (16), and compute the normalization factor as described in Appendix B.

(3) Add up the contributions of the order n_i.

It can be seen that, this method no longer deals with individual acoustical paths but works globally order by order. The computation time needed to calculate the reverberant tail even for high orders is therefore very short compared to the first parts.

E. Some tests

The proposed method has been tested by comparison between the different approaches using visual inspection of the impulse response and listening tests and by comparison between computed binaural responses with those measured in real rooms. The results of these tests are roughly summarized here.

For low orders, it can be considered that the geometrical approach provides the exact results if the spatial sampling agrees with the choosen order n_{geo}. Practically, this approach is limited to orders equals to 4 or 6 as regards to the computation time. The localization is quite good but the lack of high-order reflections imply a cutoff impression when dealing with reverberant hall. In Figs. 6 and 7, the result of the two methods are compared. Figure 6(a) and (b) shows the right- and left-impulse responses obtained by running the geometrical approach up to order 8 on a rectangular room. In Fig. 7(a) and (b) the pseudostatistical approach is used from order 5 to order 8. The results are very closed except that the pseudostatistical method gives more regular responses. There is neither an abrupt transition nor a gap between the two approachs and the listening tests give very similar impression. The pseudostatistical method provides good results even for high orders but the computation time problem implies the use of the statistical method for orders greater than 10.

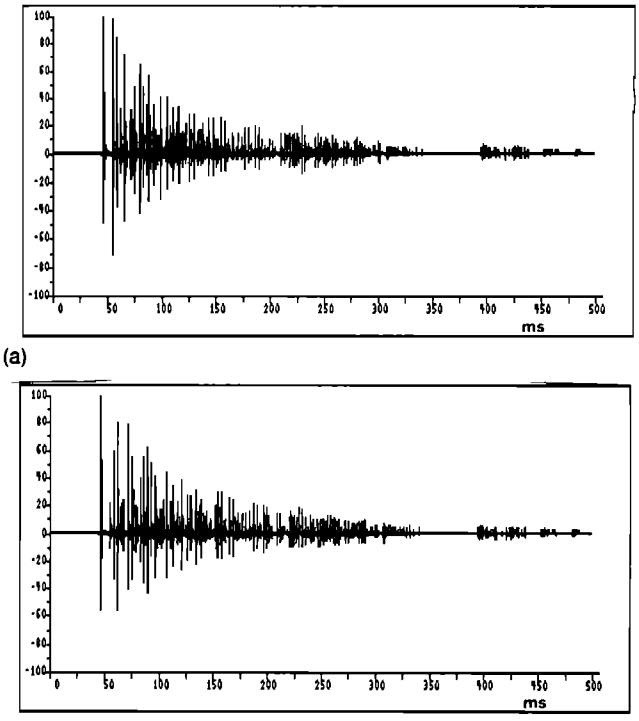

(a)

(b)

FIG. 6. (a) Right- and (b) left-ear impulse responses estimated with the geometrical approach up to order 8.

Figures 8 and 9 show the comparison between the pseudostatistical and the statistical approaches. The results are rather similar for a consequent computation time saving. Some criteria such as reverberation time have been

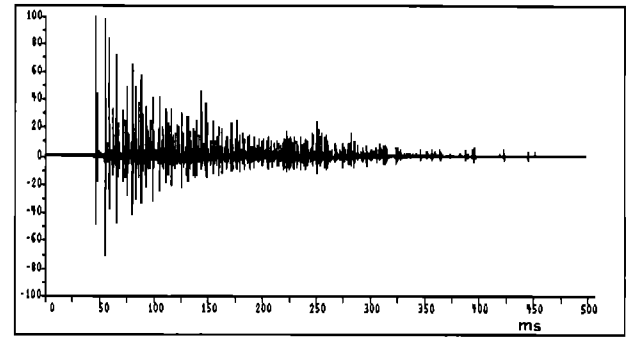

(a)

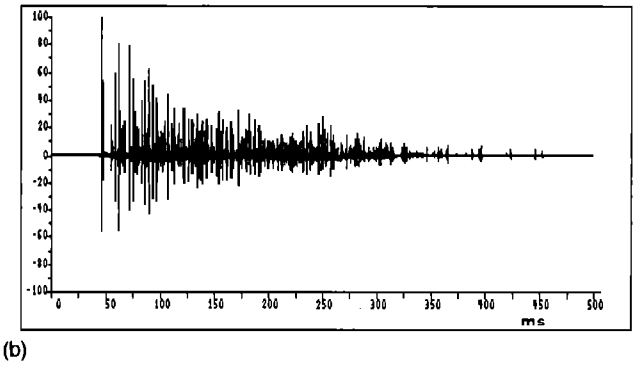

(b)

FIG. 7. (a) Right- and (b) left-ear impulse responses estimated with the geometrical approach (up to order 5) and pseudostatistical approach (orders 6 to 8).

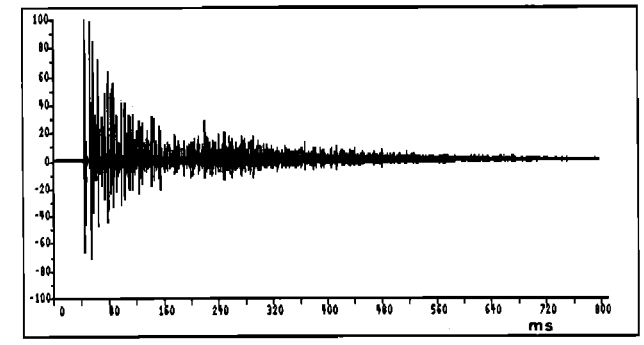

(a)

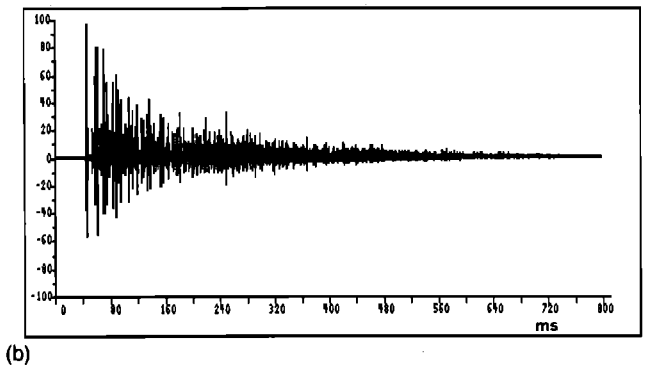

(b)

FIG. 8. (a) Right- and (b) left-ear impulse responses estimated with the geometrical approach (up to order 5) and the pseudostatistical approach (orders 6 to 20).

simultaneously estimated on measured impulse response and simulated impulse response. They were quite identical. Once again, there is a nice transition between the different approaches.

The last figures provide some comparisons between

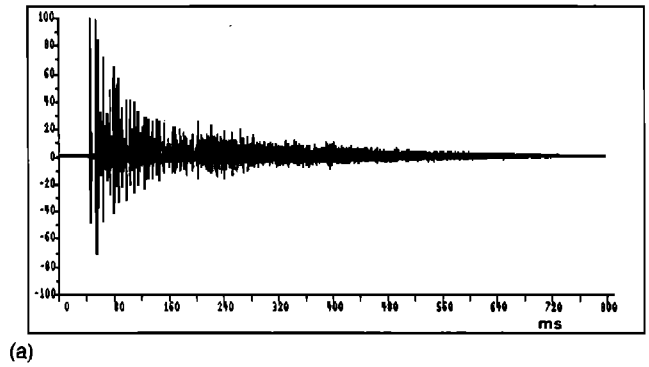

(a)

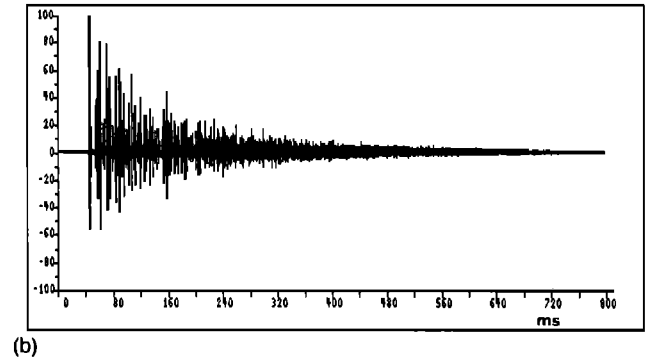

(b)

FIG. 9. (a) Right- and (b) left-ear impulse responses estimated with the geometrical approach (up to order 5), the pseudostatistical approach (orders 6 to 10) and the statistical approach (orders 11 to 20).

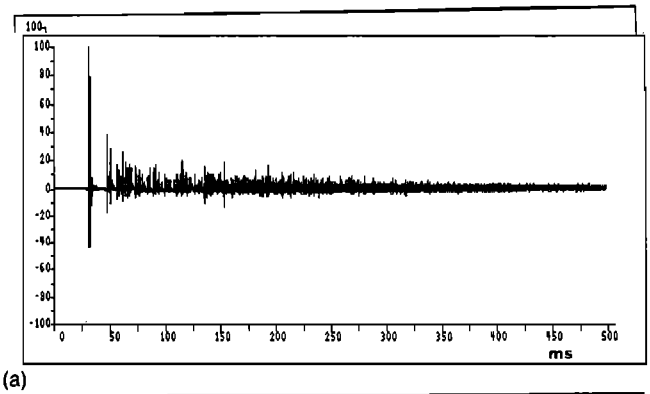

(a)

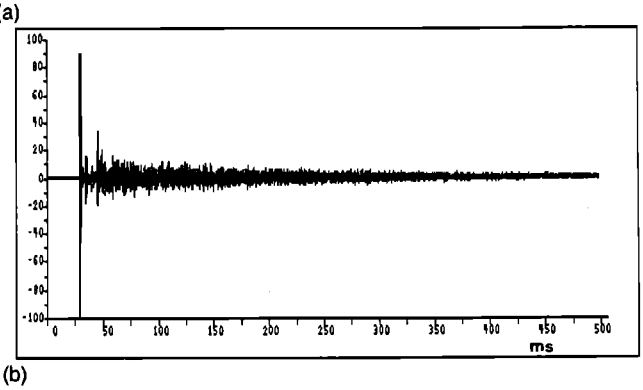

(b)

FIG. 10. (a) Predicted and (b) measured right-ear impulse responses.

computed impulse responses and those measured in the real room presented in Fig. 4(c) (Olivier Messiaen Hall in Grenoble, 320 seats, 2200 m^3).

Figure 10 shows the predicted impulse response (a) and the measured response (b) for this real hall. The auditor looks toward the source and the same measurement system (electret capsule microphones located at the ear canal entrances) as for the measurement of the HRTF is used. Figure 11(a) and (b) shows the corresponding integrated echogram with a 35-ms exponential window.

The results are rather similar except that the second path which appears on the measured response near 35 ms have been missed on the predicted response. (It can be explained by some diffraction effect on the large rectangular unit which separates the stage from the audience.) Some lack of diffusion can be seen on the geometrical beginning of the response. But the octave-band reverberation times are quite correct and the listening spatial impression of the hall is fully realistic.

IX. CONCLUSION

A new method of binaural impulse response prediction has been presented which is based on both geometrical and statistical processes. The direct sound and the early reflections are calculated according to a geometrical method and the reverberant part is calculated by using a statistical reverberant process. The main advantage of this method compared to existing electronic reverberators lies in the strong link with the real room. The exact reverberation with the right coloration can then be produced. The use of a head directivity in the propagation process provides a realistic spatial impression. As the angle between two cone axes in the geometrical algorithm cannot be as thin as

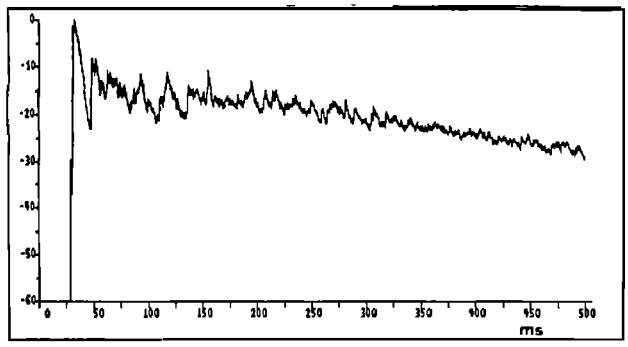

(a)

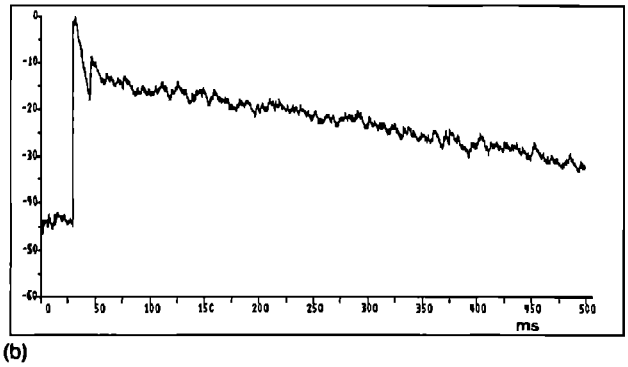

(b)

FIG. 11. 35-ms integrated echogram of the (a) predicted and (b) measured right-ear responses.

desired (because of the computation time), the image-source characteristics become bad when the reflection order increases (for instance the time density of the image sources). The proposed algorithm compensates for this drawback since it uses extrapolated characteristics from those obtained for low values of the reflection order. Impulse responses can be predicted up to reflection order equal to 100 without prohibitive computation time. This method is a very tractable way to help the acoustical planning of a hall or to investigate in auditory spaciousness or in artificial sound field generation. Some improvements can be considered especially in the accuracy of the ears transfer functions measurement and in the introduction of diffusion process in the geometrical part of the algorithm.

APPENDIX A: DETERMINATION OF THE PROBABILITY DISTRIBUTION OF THE DISTANCE r FOR AN nth-ORDER PATH WHICH REACHES THE LISTENER

Let $P_n(r)$ denotes this distribution. Let T_n be the class of all the nth-order paths and T_n^L the subclass of the n-order paths which reach the listener. It can be shown (central limit theorem—see Ref. 19) that the distance distribution function of a T_n path obeys a Gaussian law $q_n(r)=N(n\bar{l},\sqrt{n}\sigma_{\bar{l}})$ where $\bar{l}$ represents the mean-free path and $\sigma_{\bar{l}}^2$ its variance for high values of n ($n>10$). This means that the probability for a T_n path to be of length between r and $r+dr$ is equal to $q_n(r)dr=N(n\bar{l},\sqrt{n}\sigma_{\bar{l}})dr$. Now the fact that this path reach the listener must be introduced. Let the expression "reaching condition" denote this fact.

The probability for a path of length r to reach the listener is proportional to r^2. (As illustrated in Fig. A1 for a rectangular room, the number of image sources distant by $d\in[r,r+dr]$ is proportional to the volume included between the two spheres, and thus to r^2.)

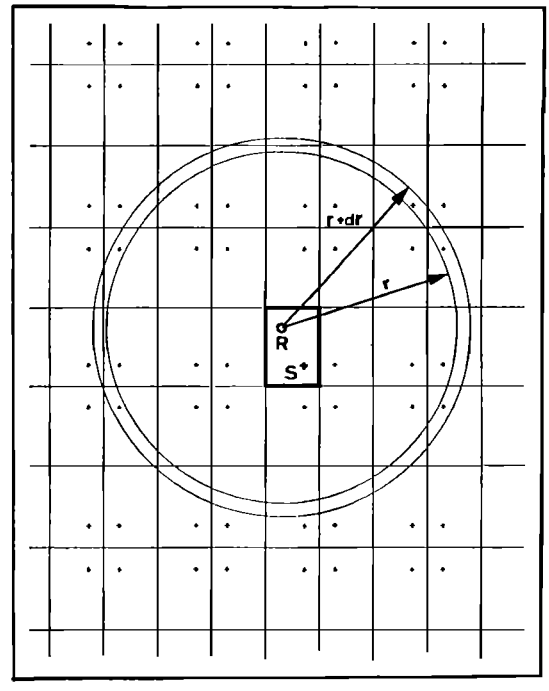

FIG. A1. Spatial distribution of image sources (rectangular room).

Now, it is assumed that the reaching condition and the condition for a ray to belong to T_n are independent. Thus

$$\begin{aligned}P_n(r)dr&=\text{prob }\{(\text{path}\in T_n^2 \text{ to be at a distance between } r \text{ and } r+dr)\}\\&=\text{prob }\{(\text{path}\in T_n \text{ and } \in[r,r+dr] \text{ and (reaching condition)}\}\\&=\text{prob }\{(\text{path}\in T_n \text{ and } \in[r,r+dr]\}\\&\quad\cdot\text{ prob }\{\text{reaching condition}/\in[r,r+dr]\}\\&=kr^2q_n(r)dr;\end{aligned}$$

$$P_n(r)=kr^2\exp\left(-\frac{1}{2}\frac{(r-n\bar{l})^2}{n\sigma_{\bar{l}}^2}\right),$$

k is given by the normalization condition,

$$\int_{-\infty}^{+\infty}P_n(r)dr=1\rightarrow k=\frac{1}{\sqrt{2\pi}\sigma_{\bar{l}}(n\sigma_{\bar{l}}^2+n^2\bar{l}^2)}.$$

APPENDIX B: NORMALIZATION OF THE STATISTICAL METHOD FOR THE ORDER n

Let $E_R^{n_{ps}}$ and $E_L^{n_{ps}}$ be the right ear and left ear energies estimated over the order n_{ps} (n_{ps}=the last order of the pseudostatistical method). The normalization process includes the following operations.

(1) Filtering of the two white noises $B_R(t)$ and $B_L(t)$, respectively, by $f_R(f)$ and $f_L(f)$:

$$f_R(f)=[1-\bar{\alpha}(f)]^{n_{ps}}[A_{n_{ps}}\bar{l}(f)]\cdot \mathrm{RE}(f),$$

$$f_L(f)=[1-\bar{\alpha}(f)]^{n_{ps}}[A_{n_{ps}}\bar{l}(f)]\cdot \mathrm{LE}(f),$$

where $A_{n_{ps}}\bar{l}(f)$ is the air absorption filter corresponding to a distance of $n_{ps}\bar{l}$, $\mathrm{RE}(f)$ is the mean right-ear filter, and $\mathrm{LE}(f)$ is the mean left-ear filter;

(2) computation of the corresponding energies E_R^n and E_L^n;

(3) filtering by $[1-\bar{\alpha}(f)]^{n-n_{ps}}$ and $A_{(n-n_{ps})}\bar{l}(f)$; and

(4) multiplying the right- and the left-ear responses, respectively, by

$$k_0^R=E_R^{n_{ps}}/E_R^n \text{ and } k_0^L=E_L^{n_{ps}}/E_L^n.$$

[1] J-P. Vian and D. Van Maercke, "Calculation of the room impulse response using a ray-tracing method," 12th ICA, Vancouver, pp. 74–77, (1986).

[2] M. R. Schroeder and B. F. Logan, "Colourless artificial reverberation," JAES 93(3), 192–197 (1961).

[3] M. R. Schroeder, "Improved quasi-stereophony and 'colourless' xartificial reverberation," JAES 33(8), 1061–1064(1961).

[4] M. R. Schroeder, "Natural sounding artificial reverberation," JAES, 219–223 (July 1962).

[5] J. A. Moorer, "About this reverberation business," IRCAM Report 17/78.

[6] C. Pösselt, J. Schröter, M. Opitz, P. L. Divenyi, and J. Blauert, "Generation of binaural signals for research and home entertainment," ICA 86.

[7] M. Morimoto and Z. Maekawa, "Effect of low frequency components on auditory spaciousness," Acustica 66(4), 190–196 (1988).

[8] J. Blauert and W. Lindemann, "Auditory spaciousness: some further psychoacoustic analyses," J. Acoust. Soc. Am. 80, 533–542 (1986).

[9] M. R. Schroeder, D. Gottlob, and K. F. Siebrasse, "Comparative study of European concert halls: correlation of subjective preference with geometric and acoustic parameters," J. Acoust. Soc. Am. 56, 1195–1201 (1974).

[10] M. Morimoto and C. Pösselt, "Contribution of reverberation to auditory spaciousness in concert halls," J. Acoust. Soc. Jpn. 10, 87–92 (1989).

[11] M. Barron, "The subjective effects of first reflections in concert halls—The need for lateral reflections," J. Sound Vib. 15, 475–494 (1971).

[12] J. Martin and J-P. Vian, "Binaural sound simulation of concert halls by a beam tracing method," 13th ICA, Belgrade, 253–256 (1989).

[13] H. E. Bass, "Absorption of sound by the atmosphere," Phys. Acoust. 17 (1984).

[14] M. Kunt, *Traité d'électricité—Volume XX—Traitement numérique des signaux* (Presses Polytechniques Romandes, Switzerland).

[15] M. Villot, "A TDS measuring system developed for a personal computer," Noise Control Eng. J., 154–158 (December 1988).

[16] J. M. Rouffet, "Description d'un système polyvalent de mesures acoustiques intégré sur micro ordinateur," 1st French Conference on Acoustics, (LYON, 1990), pp. 1063–1066.

[17] E. Parzen, "Multiple time series modeling," in *Multivariate Analysis, Vol. 2*, edited by P. R. Krishraiah (Academic, New York, 1969), Vol. 2.

[18] J. Pujolle, "Nouveau point de vue sur l'acoustique des salles," Revue d'Acoustique 18, 21–25 (1972).

[19] H. Kuttruff, *Room Acoustics* (Applied Science, London), 2nd ed.

[20] H. Lehnert and J. Blauert, "Principles of binaural room simulation," Appl. Acoust. 36, 259–291 (1992).

[21] Y. Ando and M. Sakamoto, "Superposition of geometries of surface for desired directional reflections in a concert hall," J. Acoust. Soc. Am. 84, 1734 (1988).

[22] J. Blauert, *Spatial Hearing—The Psychophysics of Human Sound Localization* (MIT, Cambridge, MA, 1983).